Electron. Mater. Lett., Vol. 10, No. 4 (2014), pp. 749-752
DOI: 10.1007/s13391-014-4007-8

Effect of Annealing on Lattice Strain and Near-Band-Edge Emission of ZnO Nanorods

Musbah Babikier, Jinzhong Wang,* Dunbo Wang, Qian Li, Jianming Sun, Yuan Yan, Wenqi Wang, Qingjiang Yu, Shujie Jiao, Shiyong Gao, and Hongtao Li

Department of Opto-electric Information Science, School of Materials Science and Engineering, Harbin Institute of Technology, Harbin 150001, China

(received date: 6 January 2014 / accepted date: 29 January 2014 / published date: 10 July 2014)

The effect of air and oxygen annealing on the structural and the optical properties of hydrothermally synthesized ZnO nanorods was investigated. After hydrothermal synthesis, the resulting ZnO nanorods were annealed in air and under an oxygen atmosphere at 370°C for 1 h. X-ray diffraction results revealed that the oxygen-annealed nanorods possessed high crystallinity with a hexagonal-wurtzite crystal structure in the (002) plane. Evaluation of strain showed a tensile lattice strain of 0.426% resulting from oxygen annealing. The photoluminescence measurements showed that the relative intensity ratio of the near-band-edge emission (NBE) to the green emission (I_{NBE}/I_{GE}) increased from ~2.6 for the as-grown ZnO nanorods to ~68.7 when the nanorods were annealed under oxygen. After annealing, a red shift of ~30 and ~44 meV in the NBE was observed for the nanorods that were annealed in air and under oxygen, respectively. This shift is attributed to the interaction between the neutral acceptors and the adsorbed oxygen atoms.

Keywords: ZnO, semiconductor, structural, luminescence

1. INTRODUCTION

Owing to zinc oxide's wide band gap of ~3.37 eV and large exciton binding energy of ~60 meV, it is a potential material for various applications including opto-electronics and catalysis.[1] The use of ZnO in commercial manufacturing is limited, however, because of the lack of *p*-type ZnO.[2] Currently, there are extensive research studies on the use ZnO nanostructures in nanodevices. ZnO nanostructures can be synthesized by different approaches such as vapor-phase growth, melt growth, and hydrothermal methods. In particular, there has been a drastic increase in interest on hydrothermally grown ZnO nanorods for different applications such as high-efficiency light-emitting diodes, solar cells, and sensitive UV detectors.[3] However, there remain challenges regarding the properties of ZnO nanorods, including a high concentration of point defects that arise during growth at low temperature. The most mentioned point defects are oxygen vacancies (V_O) and zinc vacancies (V_{Zn}) because they exist in high densities. Calculations based on density functional theory showed that V_O has a very low concentration under O-rich conditions and do not contribute to the *n*-type conductivity in *n*-ZnO.[4] On the other hand, first-principles calculations revealed that V_{Zn} exists in a high concentration even under equilibrium conditions.[4] Moreover, V_{Zn} has a transition level that is 0.87 eV above the valence-band maximum (VBM). Therefore, a transition involving this energy level would result in a broad, green luminescence band. Generally, the origin of the UV emission is commonly assigned to the free-exciton recombination process, while the source of visible emission is attributed to both intrinsic and extrinsic defects.[5] To gain in-depth understanding of the luminescence spectra of ZnO nanorods, different attempts have been made by considering insitu and post-growth treatments. Post-growth treatment to enhance the desired properties has received more attention. In particular, annealing of ZnO under an oxygen atmosphere has shown remarkable influence on its luminescence spectrum, whereas both the near-band-edge and the defect related emissions are found to be clearly affected.[6] In the study reported her, ZnO nanorods were synthesized using the hydrothermal method on a quartz substrate seeded with a ZnO thin film. An attempt to explore the effect of annealing atmosphere and temperature was made, where remarkable enhancement of UV emission owing to oxygen annealing was observed. The x-ray diffraction (XRD) measurements showed an improvement in the crystal structure due to annealing, which is attributed to the adsorption of oxygen in the ZnO crystal lattice.

*Corresponding author: jinzhong_wang@hit.edu.cn

2. EXPERIMENTAL PROCEDURE

A two-step method to synthesize ZnO nanorods on a quartz substrate was adopted. The synthesis process began with the deposition of a 120-nm-thick ZnO seed layer on a quartz substrate using radio-frequency (RF) magnetron sputtering of a ZnO target (99.999%) at room temperature. The sputtering details can be found in our previous report.[7] ZnO nanorods were synthesized by a simple hydrothermal method. Zinc acetate dihydrate ($C_4H_6O_4Zn.2H_2O$) and hexamethylenetetramine ($(CH_2)_6N_4$) in equimolar concentrations (0.025 M) were mixed together with 100 mL of de-ionized water in a conical flask and magnetically stirred for 10 min to obtain a homogeneous aqueous solution. The quartz substrate with the seed layer was transferred into the conical flask and placed face-down. The flask containing the aqueous solution was placed in a combusting water-bath deposition system where the nanorods were synthesized at 85°C for 90 min. After the synthesis process, the as-grown nanorods were soaked in de-ionized water several times to eliminate un-reacted materials and dried in a standard oven at 60°C for 2 h. The sample was cut into three parts (samples a, b, and c). The nanorods were then annealed in air (sample b) and under an oxygen atmosphere (sample c) at 370°C for 1 h.

The morphology of the synthesized nanorods was investigated using a scanning electron microscope (SEM; Helios Nanolab 600i, FEI). XRD measurements were carried out with a Rigaku D/Max-B x-ray diffractometer with Cu K_α radiation. Photoluminescence (PL) spectra at room temperature were recorded using a He-Cd laser at an excitation wavelength of 325 nm. Transmittance measurements were acquired by a UV-vis spectrophotometer (UV 1700PC, Shanghai Phenix Optical Scientific Instrument).

3. RESULTS AND DISCUSSION

3.1 Morphology

Top-view SEM images of the as-grown, air-annealed, and oxygen-annealed ZnO nanorods are shown in Fig. 1(a-c). It can be seen that all nanorods possessed flat surfaces with hexagonal cross sections, indicating a hexagonal-wurtzite crystal structure. Moreover, the morphology of the ZnO nanorods did not show any obvious changes as a result of annealing. The average nanorod diameter for all samples varied between 50 and 150 nm, taking into account that there were few nanorods with an average diameter below 50 nm. Additionally, the nanorods in all samples showed non-uniform vertical alignment and low density, possibly because of the large diameter.

3.2 Crystal structure

XRD measurements of the as-grown, air-annealed, and oxygen-annealed ZnO nanorods are shown in Fig. 2. The as-grown nanorods exhibited weak reflections from the (002) plane at 34.40° and the (103) plane at 62.75°. The annealed samples showed strong reflections from the (002) plane along with two weak peaks at 63.2° and 72.52°, which correspond to reflections from the (103) and (004) planes, respectively. It can be observed that the intensity of the (002) peak increased when the nanorods were annealed in air at 370°C and increased remarkably for the nanorods that were annealed under oxygen at the same temperature, indicating the reduction of the crystallographic defects by annealing.

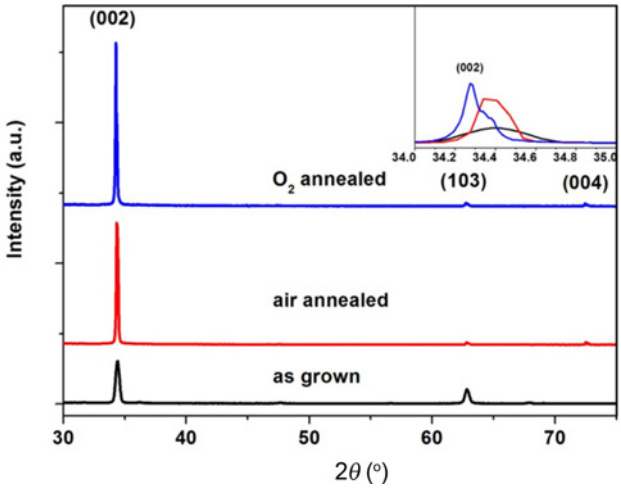

Fig. 2. XRD patterns of ZnO nanorods. The inset shows the shift of the (002) peak.

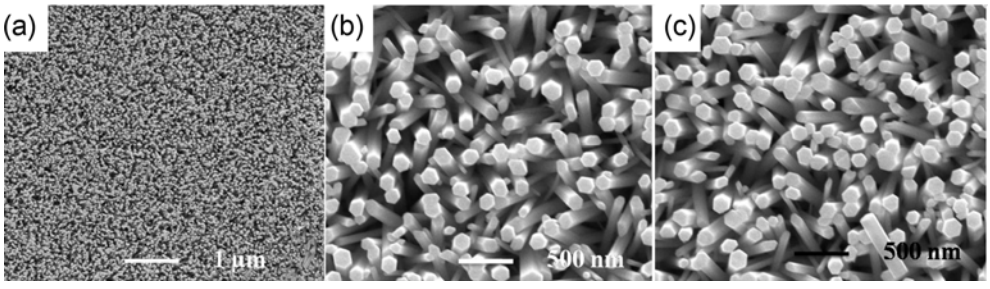

Fig. 1. Surface morphology of ZnO nanorods:(a) as-grown nanorods, (b) nanorods annealed in air, (c) nanorods annealed under an oxygen atmosphere.

Table 1. Summary of crystal properties of the as-grown and oxygen-annealed ZnO nanorods.

Sample	Annealing	d (Å)	C (Å)	FWHM (°)	D (nm)	ε_z (%)	2θ
a	As grown	2.6049	5.2088	0.319	4.7	0.074	34.40
b	Air annealed	2.6063	5.2126	0.175	8.6	0.126	34.36
c	O_2 annealed	2. 6141	5.2282	0.163	9.4	0.426	34.26

The strong x-ray intensity from (002) plane confirms the growth of the nanorods along the *c*-axis perpendicular to the substrate. On the other hand, the weak reflections at 63.2° and 72.52° could be attributed to either the inclined nanorods or the presence of crystal defects. According to the standard reference data (JCPDS No. 36e1451), all peaks in all samples were assigned to the hexagonal-wurtzite crystal structure of ZnO. Moreover, the stronger (002) peak of the air- and oxygen-annealed nanorods showed a shift toward lower angles relative to the as-grown ZnO nanorods, indicating an increase in the lattice constant *c*. The lattice parameters (*c* and *d*) of the wurtzite structure along the (002) plane were calculated from ($n\lambda = 2d_{hkl}\sin\theta$) and ($c = 2d$), where n, λ, d_{hkl}, and θ are the diffraction order, x-ray wavelength, plane distance, and diffraction angle, respectively. The parameters are listed in Table 1. The lattice constant *c* increased when the nanorods were annealed in air and increased further when the nanorods were annealed under an oxygen atmosphere. This result is expected since the position of the (002) peak of the annealed nanorods shifted to a lower angle relative to the as-grown nanorods.

The as-grown nanorods showed higher full width at half maximum (*FWHM*), while the annealed samples (samples b and c) showed small *FWHM* values along the *c*-axis, indicating that annealing in air and under oxygen at 370°C improved the nanorods' crystallinity. The *FWHM* values were substituted into Scherrer's equation[8] to estimate the crystallite size (*D*). As expected, the as-grown ZnO nanorods exhibited lower crystallite size compared to the annealed nanorods (Table 1). Moreover, the lattice strain (ε_z) can be calculated using Eq. (1),

$$\varepsilon_z = \frac{c - c_0}{c_0} \times 100\,, \tag{1}$$

where *c* is the lattice constant of the ZnO nanorods calculated from the XRD measurements and c = 5.206 Å is the lattice constant of the standard unstrained ZnO. All samples showed tensile strain, with the annealed nanorods exhibiting higher tensile strain relative to the as-grown nanorods.

3.3 Photoluminescence properties

Figure 3 shows the photoluminescence (PL) spectra acquired at room temperature. It can be seen that all samples exhibited two dominant emission bands. The first emission band was centered at 376 nm (near-band-edge emission), which is commonly ascribed to the radiative recombination process

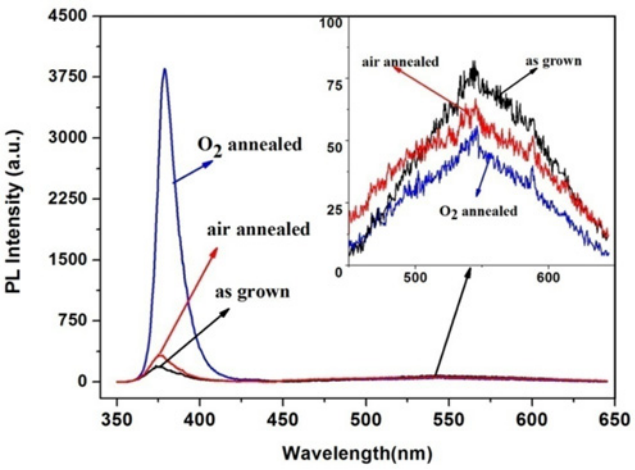

Fig. 3. Room temperature PL spectra of ZnO nanorods. The inset shows the green emission intensity.

by free excitons. The second band is a broad green emission band centered at 540 nm. Obviously, the UV emission increased slightly when the nanorods were annealed in air and was enhanced significantly when the ZnO nanorods were annealed at 370°C for 1 h under an oxygen atmosphere, where the relative intensity ratio ($R = I_{NBE}/I_{Vis}$) increased from 2.6 (for the as-grown nanorods) to 3.2 when the nanorods were annealed in air and to 68.7 for the oxygen-annealed nanorods. The enhancement in the UV emission can be explained by the effect of strain on the band structure. It is evident that annealing under oxygen resulted in tensile strain (Table 1), which had a significant impact on the valence band maximum. The tensile strain could bend the band upward, thereby allowing a large density of holes to accumulate at the top of valence band, which could increase the luminescence quantum yield near the band edge. Additionally, the UV emission peak showed red shifts of ~30 and ~44 meV when the ZnO nanorods were annealed in air and under oxygen, respectively. The red shift of the NBE may have resulted from either the interaction between the neutral acceptors and adsorbed oxygen atoms or from the effect of tensile strain on the VBM.[9] The origin of the green-light emission from ZnO has been a fundamental question in many research debates, with the emission attributed to several origins including point defects (oxygen and zinc vacancies) and Cu impurities.[9-11] Apparently, the green emission intensity decreased slightly when the nanorods were annealed in air and decreased more after

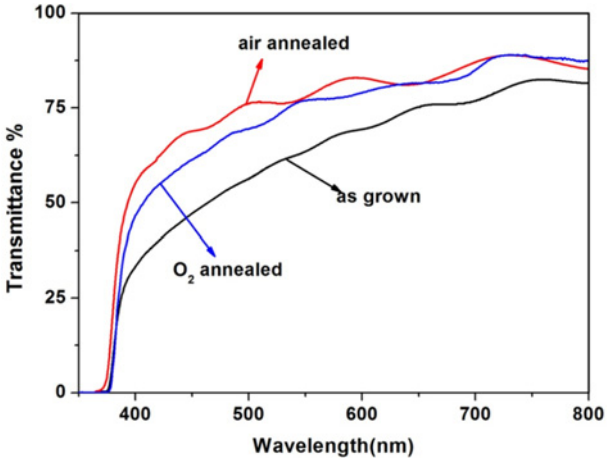

Fig. 4. The average total transmittance spectra of ZnO nanorods.

oxygen annealing. This result indicates that the as-grown nanorods contained a rather high concentration of defects, which is consistent with the XRD analysis. Recently, theoretical calculations have revealed that the zinc vacancy has a transition level at 0.87 eV above the VBM, and hence, transition involving this level would result in a structureless green emission band at about 2.5 eV.

3.4 Transmittance

The average total transmittance spectra of the as-grown, air-annealed, and oxygen-annealed ZnO nanorods are shown in Fig. 4. It is evident that all samples were transparent in the visible range and exhibited a sharp absorption edge at around 378 nm. The transmittance increased from 75% for the as-grown nanorods to ~88% when the nanorods were annealed under air and oxygen (samples b and c). It appeared that the nanorods annealed under oxygen were less transparent than the nanorods annealed in air in the wavelength range of 400 - 550 nm. ZnO nanorods that were annealed at 370°C in air exhibited a blue shift in the fundamental absorption edge around 378 nm relative to the as-grown and oxygen-annealed ZnO nanorods, indicating a shift in the band gap. It was observed that the transmittance spectra for the annealed samples (samples b and c) behaved like standing waves; this is due to the interference between the incident light and the light reflected at the interface between the ZnO seed layer and the nanorods. This behavior was more pronounced when the nanorods were annealed in air. In general, the transmittance spectra were affected by various factors including nanorod dimensions, density of nanorods, alignment of nanorods, scattering centers that were formed in situ, and concentration of defects.[12]

4. CONCLUSIONS

In conclusion, we explored the effect of air and oxygen annealing at 370°C on the structural and the optical properties of the hydrothermally grown ZnO nanorods. XRD studies revealed that oxygen annealing induced a tensile strain of 0.426% owing to the adsorption of oxygen on the ZnO crystal lattice. SEM images confirmed that the nanorods were grown perpendicular to the substrate along the*c*-axis and had a diameter that varied between 50 and 150 nm. The PL characteristics showed significant increase in the near-band-edge emission intensity, where the relative intensity ratio ($R = I_{NBE}/I_{Vis}$) increased from 2.6 for the as-grown nanorods to 68.7 after oxygen annealing. The red shift of the NBE is attributed to the interaction between the neutral acceptors and the adsorbed oxygen atoms

ACKNOWLEDGMENTS

This work has been partly supported by the Program for New Century Excellent Talents in University (NCET-10-0066), an 863 project grant (2013AA031502), and Project No. 2011RFLXG006.

REFERENCES

1. U. Ozgur, Y. I. Alivov, C. Liu, A. Teke, M. A. Reshchikov, S. Dogan, and H. Morkoc, *J. Appl. Phys.* **98**, 041301 (2005).
2. C. H. Park, S. B. Zhang, and S. H. Wei, *Phys. Rev. B*. **66**, 073202 (2002).
3. W. Benjamin, Z. Zhengzhi, L. Yinhu, and D. Yulin, *Nanoscale* **2**, 1573 (2010).
4. A. Janotti and C. van de Walle, *Phys. Rev. B.* **76**, 165202 (2007).
5. Y. K. Su, S. M. Peng, L. W. Ji, C. Z. Wu, W. B. Cheng, and C. H. Liu, *Langmuir* **26**, 603 (2010).
6. P. K Samanta, S. K. Patra, and P. R. Chaudhuri, *Int. J. Nanosci. Nanotechnol.* **81**, 20865 (2009).
7. M. Babikier, D. Wang, J. Wang, Q. Li, J. Sun, Y. Yan, Q. Yu, and S. Jiao, *J. Mater. Sci.: Mater. Electron.* **25**, 157 (2014).
8. G. Sanon, R. Rup, and A. Mansingh, *Thin Solid Films* **190**, 287 (1989).
9. B. Yu, X. Xu, S. Zhuang, J. Pan, and J. Hu, *Mater. Lett*. **82**, 145 (2012).
10. R. Dingl, *Phy. Rev. Lett.* **23**, 579 (1969).
11. M. D. McCluskey and S. J. Jokela, *J. Appl. Phys.* **106**, 071101 (2009).
12. S. Lin, H. Hu, W. Zheng, Y. Qu, and F. Lai, *Nanoscale. Res. Lett.* **8**, 158 (2013).